Accepted Manuscript

Novel hybrids of brefeldin A and nitrogen mustards with improved antiproliferative selectivity: Design, synthesis and antitumor biological evaluation

Tong Han, Kangtao Tian, Huaqi Pan, Yongxiang Liu, Fanxing Xu, Zhanlin Li, Takahiro Uchita, Ming Gao, Huiming Hua, Dahong Li

PII: S0223-5234(18)30235-6

DOI: 10.1016/j.ejmech.2018.02.088

Reference: EJMECH 10265

To appear in: *European Journal of Medicinal Chemistry*

Received Date: 15 November 2017

Revised Date: 10 February 2018

Accepted Date: 28 February 2018

Please cite this article as: T. Han, K. Tian, H. Pan, Y. Liu, F. Xu, Z. Li, T. Uchita, M. Gao, H. Hua, D. Li, Novel hybrids of brefeldin A and nitrogen mustards with improved antiproliferative selectivity: Design, synthesis and antitumor biological evaluation, *European Journal of Medicinal Chemistry* (2018), doi: 10.1016/j.ejmech.2018.02.088.

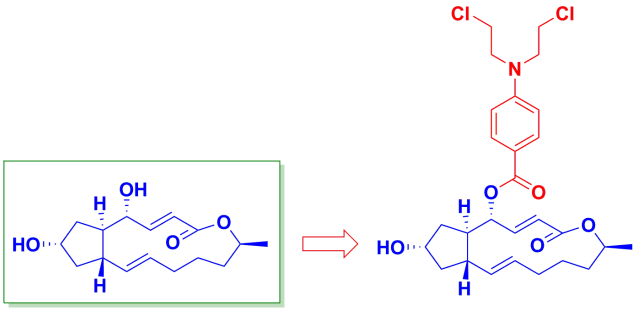

BFA, 1

11a

- Arrested cell cycle at the G1 phase
- MMP ($\Delta\psi_m$) ↓
- Mitochondria-dependent apoptotic pathway

Bel-7402: IC_{50} = 0.024 μM
Bel-7402/5-FU: IC_{50} = 0.82 μM
L-O2: IC_{50} < 0.001 μM

Bel-7402: IC_{50} = 0.25 μM
Bel-7402/5-FU: IC_{50} = 0.84 μM
L-O2: IC_{50} = 9.74 μM
$SI_{L\text{-}O2/Bel\text{-}7402}$ = 39

Novel hybrids of brefeldin A and nitrogen mustards with improved antiproliferative selectivity: design, synthesis and antitumor biological evaluation

Tong Han[a,1], Kangtao Tian[a,1], Huaqi Pan[b,1], Yongxiang Liu[c], Fanxing Xu[c], Zhanlin Li[a], Takahiro Uchita[d], Ming Gao[d], Huiming Hua[a], Dahong Li[a,*]

[a]*Key Laboratory of Structure-Based Drug Design & Discovery, Ministry of Education, and School of Traditional Chinese Materia Medica, Shenyang Pharmaceutical University, 103 Wenhua Road, Shenyang 110016, PR China*

[b]*Shenyang Institute of Applied Ecology, Chinese Academy of Sciences, 72 Wenhua Road, Shenyang 110016, PR China*

[c]*Wuya College of Innovation, Shenyang Pharmaceutical University, 103 Wenhua Road, Shenyang 110016, PR China*

[d]*School of Pharmaceutical Sciences, Mukogawa Women's University, 11-68 Koshien, Nishinomiya 663-8179, Japan*

[*]Corresponding author.

Tel: +86 2423986465 (D. Li); E-mail addresses: lidahong0203@163.com (D. Li).

[1]These authors contributed equally to this work.

ABSTRACT

A series of novel conjugates of brefeldin A (**11a−c**, **12a−c** and **13a−c**) were obtained by introducing a variety of nitrogen mustards at 4-OH or 7-OH position to explore more efficacious and less toxic antitumor agents. The antiproliferative activities were tested against three cancer cell lines (HL-60, PC-3 and Bel-7402) and one multidrug resistant cell line Bel-7402/5-FU. Among them, compound **11a** was the strongest derivative with IC_{50} values of 4.48, 9.37, 0.2 and 0.84 μM, respectively, and more potent than nitrogen mustards. Though the antiproliferative potency was weaker than the lead compound brefeldin A, **11a** displayed lower toxicity than brefeldin A (IC_{50} < 0.001 μM) with an IC_{50} of 9.74 μM against normal human liver L-O2 cells, showing good selectivity between normal and malignant liver cells. The mechanism studies confirmed that **11a** could induce apoptosis, arrest cell cycle at the G1 phase and lead to mitochondrial dysfunction in Bel-7402 cells at submicromolar concentrations. Furthermore, **11a** induced the intrinsic apoptotic mitochondrial pathway in Bel-7402 cells, evidenced by the enhanced expression of the pro-apoptotic protein Bax, cyto-*c* and p53, and the reduced expression of the anti-apoptotic protein Bcl-2. The caspase-9 and -3 levels were also up-regulated.

Keywords: brefeldin A, antiproliferative activity, nitrogen mustards, selectivity, hybrids

1. Introduction

Cancer, the second cause of mortality in the world, is continuing to be a major health problem in developing countries [1,2]. According to recent statistics, cancer incidence and mortality have been increasing in China and this situation will become even more severe in the future with the rapidity of population aging process [3]. Therefore, discovering new anticancer agents remains of critical importances.

Natural products have played prominent roles for drug discovery and cancer therapy [4,5]. Brefeldin A (BFA, **1**) (Figure 1) is a 16-membered macrolide antibiotic which was first isolated from *Penicillium decumbens* [6]. It shows a wide variety of biological properties, including antitumor [7,8], antifungal [9], antimitotic [10] and antiviral effects [11]. The potent antiproliferative activity of BFA was tested by the National Cancer Institute's 60 (NCI-60) cancer cell line assay with the mean graph midpoint (MGM) GI_{50} value of 40 nM [12]. Due to its attractive biological activities and the potential as a lead for anticancer drug development, BFA has been a target of study for numerous chemists and pharmacologists [13−15]. Its possible mechanisms were disclosed by a number of important discoveries. Especially, BFA could block the secretory process in eukaryotic cells by interfering the endoplasmic reticulumto Golgi membrane traffic, causing the disassembly of Golgi apparatus and redistribution of Golgi-apparatus proteins into the endoplasmic reticulum [16], contributing to its activities. Moreover, it could induce apoptosis in a wide variety of human cancer cells, such as ovarian carcinoma cells by activating the mitochondrial pathway and caspase-8 [17], neuroendocrine tumor and prostatic cancer cells via a p53-independent mechanism [18], as well as breast cancer cells by decreasing the level of CD44 and anti-apoptotic proteins Bcl-2 and Mcl-1 [19]. Despite its potentials to be a cancer chemotherapeutic agent, BFA faces some major limitations, such as

undesirable drug-like properties and low selectivity between tumor and normal cells [20,21].

The structural modification of BFA focused on *α,β*-unsaturated lactone and the C4 and C7 hydroxyl groups. The cytotoxic activity of BFA was to reduce without carbon-carbon double bond or lactone bond [22]. Methylation or oxidation at C4 and C7 hydroxyl groups also decreased the antiproliferative activities [23]. The sulfide and sulfoxide derivatives of BFA displayed promising antitumor effects in vitro and in vivo. Perhaps, after drug metabolism, an intact BFA pharmacophore generated [24]. And the ester derivatives at the C4 and C7 hydroxyl groups of BFA, such as **A** and **B** (Figure 1), also exhibited strong cytotoxicity [12]. Moreover, a series of analogues of modified C15 methyl group were reported. Most of the analogues exhibited significant biological activities, especially when the methyl group was replaced by vinyl (**C**) or phenemyl (**D**) groups [25] (Figure 1). Therefore, the strategy to develop novel BFA derivatives by rational modification is effective.

Nitrogen mustards are DNA alkylating agents which have been widely used in cancer chemotherapy with the advantages of broad spectrum and strong potency of antitumor activity [26]. Combining nitrogen mustards with natural products is a good way to develop novel antitumor agents (**E**−**H**) [27−30] (Figure 2). Herein, we describe the design and synthesis of a series of novel BFA-nitrogen mustard conjugates with cytostatic activity and improved antiproliferative selectivity between malignant and normal cells.

2. Result and Discussion

2.1. Chemistry

The BFA was isolated from the fermentation liquor and mycelium of

Eupenicillium brefeldianum, and characterized by ^{1}H NMR, ^{13}C NMR, high-resolution mass spectra, X-ray crystal structure analysis and optical rotation. The synthesis of the new BFA derivatives is outlined in Schemes 1 and 2. The nitrogen mustard intermediates were prepared as depicted in Scheme 1. The benzoic acid mustard **4** was prepared according to the literature [31]. Simply, reaction of **2** with ethylene oxide in 25% acetic solution gave **3**, then treatment of **3** with phosphorus oxychloride followed by hydrolysis of the ester with concentrated hydrochloric acid obtained **4**. Esterification of **5** in dry methanol and the presence of $SOCl_2$ led to ester **6** in quantitative yield, and subsequent reaction of **6** with succinic anhydride provided melphalan derivative **7** (Scheme 1).

In order to get the ester derivatives only at C4, the 4,7-OH groups were firstly protected with *tert*-butyldimethylsilyl (TBS) groups using *tert*-butyldimethylsilyltriflate (TBSOTf) and 2,6-lutidine in dichloromethane (DCM). The TBS group on 4-OH of **8** was removed by *tert*-butylammonium fluoride (TBAF) in THF to obtain the intermediate **9** (Scheme 2). Reacting compound **9** with intermediates **4**, **7** or chlorambucil in the presence of DMAP and 1-ethyl-3-(3-dimethylaminopropyl) carbodiimide hydrochloride (EDCI) afforded **10a**−**c**. The derivatives **11a**−**c** were got from **10a**−**c** by the deprotection with TBAF in THF. Target compounds **12a**−**c** and **13a**−**c** were prepared from the combination of **4**, **7** or chlorambucil and BFA in the presence of DMAP and EDCI in DCM, followed by column chromatography on silica gel using petroleum ether-ethyl acetate (V : V = 2 : 1). The structures of all the derivatives were confirmed by ^{1}H NMR, ^{13}C NMR and high resolution mass spectrum (HR-MS).

2.2. Biological evaluation

2.2.1 Cytotoxic activity and structure-activity relationships analysis

The cytotoxic activities of target hybrids **11a−c**, **12a−c** and **13a−c** against three human cancer cell lines (HL-60 human leukemic cell line, PC-3 human prostatic cancer cell line and Bel-7402 hepatocellular carcinoma cell line), the multidrug resistant cell line Bel-7402/5-FU and the human normal hepatic cell line (L-O2) were screened and compared with lead compound BFA (**1**), nitrogen mustards (chlorambucil, **4** and **7**) and positive control 5-fluorouracil (5-FU) in each panel. As shown in Table 1, almost all the target compounds showed cytotoxic activities against one or more cell lines. For instance, compounds **11a**, **12a**, **13a**, **11b**, **12c** and **13c** exhibited cytotoxic activities against three cancer cell lines with IC_{50} values ranging from 0.25 to 18.54 μM. **12b** showed antiproliferative activities against PC-3 and Bel-7402 cells with IC_{50} values of 6.84 and 4.86 μM, respectively, and **13c** with IC_{50} values of 9.37 and 4.85 μM against HL-60 and Bel-7402 cells, respectively. The benzoic acid mustard combined compounds (**11a**, **12a** and **13a**) were more potent than those with chlorambucil (**11b**, **12b** and **13b**) and melphalan (**11c**, **12c** and **13c**). In addition, 4-OH linked hybrids **11a** and **11b** showed stronger cytotoxic effects than 7-OH linked **12a** and **12b,** and 4,7-OH derivatives **13a** and **13b**. It is worth noticing that all the hybrids exhibited more potent inhibitory activities (IC_{50} 0.25−7.25 μM) than nitrogen mustards, and some of them showed superior cytotoxic activities to 5-FU (IC_{50} 18.49 μM) against Bel-7402 cells. In Bel-7402/5-FU cell line, all the compounds exhibited stronger activities (IC_{50} 0.84−15.63 μM) than nitrogen mustards and 5-FU (IC_{50} > 80 μM). Especially, **11a** displayed the most potent cytotoxic activity among all the derivatives with IC_{50} values of 0.25 μM against Bel-7402 cells and 0.84 μM against Bel-7402/5-FU cells.

To investigate whether the hybrids exhibited selective antiproliferative activities between normal and malignant liver cells, **11a−c**, **12a−c** and **13a−c** were tested

against human normal liver L-O2 cells with BFA and nitrogen mustards as control. The results were listed in Table 1. Compared with BFA (IC_{50} < 0.001 μM), all the targeted compounds showed lower antiproliferative activities against L-O2 cells with IC_{50} values from 4.57 to 29.87 μM. In particular, **11a**, the most potent one against Bel-7402 and Bel-7402/5-FU cell lines, showed low toxicity against L-O2 cells with the IC_{50} value of 9.74 μM plus good selective index (SI). These results encouraged us to further investigate the possible cellular mechanisms of **11a** in Bel-7402 cell line.

*2.2.2 Stability of **11a***

To verify that if compound **11a** was easy to hydrolyze and release free BFA, the stability of compound **11a** was studied in DMEM culture media supplemented with FBS under cell-free conditions (cell-free cDMEM) [32]. The results of HPLC analysis were summarized in Figure 3. It could be observed that compound **11a** was stable in DMEM culture media with no detectable hydrolyzed BFA within 24 h.

2.2.3 Cell cycle analysis

To determine whether the cell cycle arrest was participated in the suppression of cell growth by **11a**, the DNA content of cell nuclei was detected by flow cytometry. Bel-7402 cells were treated with **11a** (0.125, 0.25 and 0.5 μM) for 72 h, stained with propidium iodide (PI) and analyzed by flow cytometry. Non-treated cells were used as control. As shown in Figure 4, cells in the G1 phase increased from 39.28% in control group to 43.80%, 54.26% and 58.17% in a concentration-dependent manner in Bel-7402 cell lines. The results revealed that **11a** caused G1 phase arrest in a concentration-dependent manner.

2.2.4 The morphological analysis by Hoechst 33258 staining

The changes of morphological features, such as cell shrinkage, chromatin condensation and nuclear membrane bleb are the characteristics of apoptotic cells [33].

Hence, to clarify whether the loss of cancer cell viability by **11a** was associated with apoptosis, we used fluorescence microscopy to observe the morphology of Bel-7402 cells stained with Hoechst 33258, after treatment with different concentrations (the same as the cell cycle test) of **11a** for 48 h. The morphological analysis, depicted in Figure 5, showed that control cells were uniformly stained with Hoechst 33258 and presented round homogeneous nuclei, without morphological changes. Bel-7402 cells, which were exposed to 0.125 and 0.25 μM **11a**, presented remarkable morphological changes, such as cell shrinkage, chromatin condensation and evident reduction in the number of adherent cells. The rupture of cell membrane and the nuclear fragmentation were evident after the treatment of 0.5 μM **11a**. These results supported the pro-apoptotic effects of **11a** in Bel-7402 cells at submicromolar concentration.

2.2.5 Cell apoptosis assay

To further confirm the apoptosis-inducing effects of **11a**, an annexin V-FITC/PI binding assay was performed. The cells were treated with different concentrations (the same as the cell cycle test) of **11a** for 72 h. Then, the cells were harvested and stained with annexin-V and PI, and the percentages of apoptotic cells were determined by flow cytometry analysis. As shown in Figure 6, the treatment of Bel-7402 cells with **11a** at the concentrations of 0.125, 0.25 and 0.5 μM resulted in cell apoptosis of 15.96%, 33.95% and 57.59%, respectively, compared to 4.47% in the control group. The results showed that **11a** caused a marked increase of the Bel-7402 cells apoptosis in a concentration-dependent manner.

2.2.6 Mitochondria membrane potential analysis

Mitochondria play a crucial role in the induction and control of apoptosis, which results in a variety of key events, including the loss of mitochondrial membrane potential and release of pro-apoptotic factors such as cytochrome *c* (cyto-*c*), Bax and

other apoptosis-inducing factors [34]. We therefore studied the effects of **11a** on mitochondrial membrane potentials in Bel-7402 cell line. The cells were treated with different concentrations (the same as the cell cycle test) of **11a** for 48 h, and the changes of mitochondrial membrane potentials were monitored by flow cytometry using the dye 5,5′,6,6′-tetrachloro-1,1′,3,3′-tetraethylbenzimidazol caebocyanine (JC-1). As shown in Figure 7, **11a** induced a concentration-dependent increase in the proportion of cells with depolarized mitochondria. This illustrated that the induction of apoptosis by **11a** was associated with the mitochondrial (intrinsic) pathways.

2.2.7 Effects on apoptosis-related proteins

Mitochondria play an essential role in cell death signal transduction, apoptotic stimuli can activate apoptosis-related proteins such as Bax (proapoptotic protein) and Bcl-2 (antiapoptotic protein) to enter mitochondria, which induce the mitochondria to release cyto-*c* and, in turn, activate the caspase-9 and -3, finally triggering the execution of apoptosis [35,36]. Hence, to determine the involvement of the mitochondria-dependent pathway in Bel-7402 cells apoptosis induced by **11a**, we examined the expression of Bcl-2 and Bax, cyto-*c*, caspase-9 and -3 activities by Western blot analysis. Moreover, the level of p53 has also been tested, the p53 tumor suppressor gene is critically involved in cell cycle regulation, DNA repair, and programmed cell death. It can also up-regulates the transcription of Bax and represses Bcl-2 transcription in the mitochondrial pathway [37,38]. As shown in Figure 8, in comparison with the control cells, **11a** induced an increase of Bax level and a reduction of Bcl-2 level in a dose-dependent fashion. Treatment with **11a** caused an accumulation of cyto-*c* in the cytosol, most probably due to the release from mitochondria (Figure 8). Then, **11a** caused a significant increase in the levels of caspase-9 and -3 compared to the control in Bel-7402 cells. These results suggested

that **11a** increased the Bax/Bcl-2 ratio, leading to the release of cyto-*c*, caspase-9 and -3 activation, which triggered the execution of apoptosis. Furthermore, **11a** also caused the up-regulation of p53 in a concentration dependent manner. Thus, **11a** induced cell apoptosis via the mitochondria-dependent pathway.

3. Conclusion

In summary, a series of novel derivatives of BFA were obtained by introducing nitrogen mustards at 4-OH and/or 7-OH. All the synthesized compounds were evaluated for their cytotoxic effects against HL-60, PC-3, Bel-7402, Bel-7402/5-FU and L-O2 cell lines. **11a** exhibited the strongest antiproliferative potency against tumor cell lines with IC_{50} values of 4.48, 9.37, 0.25 and 0.84 μM, respectively. **11a** also displayed much lower cytotoxicity than BFA against L-O2 cells with the selective index (SI) of 38.9. Further mechanistic studies revealed that **11a** induced apoptosis and G1 phase arrest in Bel-7402 cells which were similar as BFA. Incubation with **11a** increased the number of cells with collapsed mitochondrial membrane potentials at low concentrations in a concentration-dependent manner. Therefore, the mitochondrial pathway would be involved in BFA derivatives-mediated apoptosis. Western blot analysis further confirmed that **11a** induced apoptosis via mitochondrial pathway, since **11a** increased the expression of Bax, cyto-*c*, caspase-9, -3 and p53, and reduced the relative levels of Bcl-2. Taken together, **11a** deserved further investigation as a potential chemotherapeutic agent for liver cancer.

4. Experimental

4.1. Chemistry

Chemicals and solvents were purchased from commercial sources. Further

purification by standard methods were employed when necessary. Melting points were determined on an XT-4 micro melting point apparatus and uncorrected. ^{1}H NMR and ^{13}C NMR spectra were recorded on a Bruker ARX-400 NMR spectrometer in the indicated solvents (TMS as internal standard): the values of the chemical shifts were expressed in δ values (ppm) and the coupling constants (*J*) in Hz. Mass spectra were obtained on Agilent 1100 Ion trap mass spectrometer. HR-MS were carried out on Agilent Q-TOF B.05.01 (B5125.2).

*4.1.1. General procedures to synthesize **9***

9 was obtained from **1** in a two-step sequence according to the literature [12]. To a solution of **1** (200 mg, 0.71 mmol) in 5 mL of anhydrous DCM at 0 ^{o}C, 2,6-lutidine (86 μL) was added. TBSOTf (250 μL, 1.0 mmol) was added dropwise to the reaction mixture, which was warmed to room temperature and stirred for 8 h. The mixture was extracted with DCM (5 mL × 3) and then dried over Na_2SO_4. The solvent was evaporated, and the crude product **8** was obtained. Then the TBS group of 4-OH of compound **8** (100 mg, 0.2 mmol) was selective deprotected by the addition of TBAF (0.2 mmol) in THF dropwise over 2 h. After remove of solvent, the mixture was purified by column chromatography (petroleum ether/ethyl acetate 2:1) to yield **9**. The chemical structure of **9** was confirmed by ^{1}H NMR data. The 4-OH and 7-OH of BFA have different chemical shift values in the ^{1}H NMR spectrum, in general, the δ_H of 4-OH is around 5.10, while the δ_H of 7-OH is around 4.50 [39]. The structure of **9** was determined because of the characteristic 4-OH signal δ_H 5.19 could be observed. *Compound **9**.* white oil, yield: 56%. ^{1}H NMR (400 MHz, DMSO-d_6): δ 7.34 (1H, dd, *J* = 15.6, 2.9 Hz, C_3-H), 5.73 (1H, m, C_{11}-H), 5.67 (1H, m, C_2-H), 5.19 (1H, m, OH), 5.13 (1H, d, C_{10}-H), 4.70 (1H, m, C_{15}-H), 4.21 (1H, m, C_7-H), 3.95 (1H, m, C_4-H), 2.35 (1H, m, C_9-H), 0.70−2.03 (29H, m, C_5, 2C_6, 2C_8, C_9, 2C_{12}, 2C_{13}, 2C_{14}-H, 6CH_3).

*4.1.2 General procedures to synthesize **11a−c**, **12a−c** and **13a−c***

To a solution of **9** (32 mg, 0.08 mmol) in 2.5 mL of anhydrous DCM, **4**, **7** and chlorambucil (0.08 mmol), EDCI (29 mg, 0.15 mmol) and catalytic amount of DMAP were added. The reaction solution was stirred for 2 h at room temperature. The mixture was poured into 10 mL of H_2O, and extracted with DCM (5 mL × 3). The organic layers were combined, washed with saturated NaCl solution, dried over anhydrous Na_2SO_4, and concentrated in vacuo. The residues were purified by chromatography on silica gel (petroleum ether-ethyl acetate 5:1) to afford **10a−c**. **10a−c** (0.06 mmol) in 2 mL of THF was mixed with TBAF (0.42 mmol) by stirring at room temperature for 20 h. The mixture was poured into 10 mL of H_2O and extracted with ethyl acetate (5 mL × 3). The organic layer was combined, washed with water and saturated NaCl solution, dried over anhydrous Na_2SO_4, and concentrated in vacuo, sequentially. The residues were purified by column chromatography (petroleum ether/ethyl acetate 2:1) to yield **11a−c**.

To a solution of **4**, **7** or chlorambucil (0.11 mmol) in 10 mL of anhydrous DCM, BFA (28 mg, 0.1 mmol), EDCI (60 mg, 0.3 mmol) and catalytic amount of DMAP were added. The reaction solution was stirred for 24 h at room temperature and quenched with 10 mL of H_2O, extracted with DCM (10 mL × 3), dried over anhydrous Na_2SO_4 and concentrated in vacuo. The crude product was purified by silica gel column chromatography (petroleum ether/ethyl acetate 2:1) to afford the title compounds **12a−c** and **13a−c**. Meanwhile, the 4-OH ^{1}H NMR signals (δ_H 5.41, 5.20, 5.19) of **12a−c** were observed, these inferred that nitrogen mustard derivatives were introduced to 7-OH of BFA.

*4.1.2.1 Compound **11a**.* Yellow oil, yield: 23%. ^{1}H NMR (400 MHz, DMSO-d_6): δ (ppm) 7.85 (2H, d, J = 8.9 Hz, Ar-H), 7.35 (1H, dd, J = 15.7, 3.2 Hz, C_3-H), 6.88 (2 H,

d, *J* = 8.91 Hz, Ar-H), 5.76 (1H, m, C_{11}-H), 5.55 (1H, dd, *J* = 15.7, 1.6 Hz, C_2-H), 5.43 (1H, m, C_{10}-H), 5.28 (1H, dd, *J* = 15.11, 9.70 Hz, C_4-H), 4.74 (1H, m, C_{15}-H), 4.57 (1H, d, *J* = 3.4 Hz, 7-OH), 4.09 (1H, m, C_7-H), 3.78−3.84 (8H, m, -NCH_2CH_2Cl), 0.76−2.62 (15H, m, C_5, $2C_6$, $2C_8$, C_9, $2C_{12}$, $2C_{13}$, $2C_{14}$-H, CH_3). ^{13}C NMR (100 MHz, DMSO-d_6): δ (ppm) 165.4, 165.1, 151.0, 149.8, 137.3, 131.7, 131.7, 130.2, 117.2, 117.0, 111.8, 111.8, 76.4, 71.8, 70.9, 52.2, 52.2, 50.0, 43.4, 43.2, 41.3, 41.3, 41.0, 33.89, 31.89, 26.85, 21.07. HRMS (ESI) *m/z* calcd for $C_{27}H_{35}Cl_2NO_5Na$ $[M+Na]^+$ 546.1784, found 546.1745.

4.1.2.2 Compound ***12a.*** Yellow oil, yield: 19%. ^{1}H NMR (400 MHz, DMSO-d_6): δ (ppm) 7.68 (2H, m, Ar-H), 7.37 (1H, m, C_3-H), 6.72 (2H, m, Ar-H), 5.74 (1H, m, C_{11}-H), 5.54 (1H, d, *J* = 15.8 Hz, C_2-H), 5.41 (1H, m, OH), 5.20−5.31 (2H, m, C_{10}-H, C_7-H), 4.73 (1H, m, C_{15}-H), 4.08 (1H, m, C_4-H), 3.48−3.81 (8H, m, -NCH_2CH_2Cl), 0.76−2.34 (15H, m, C_5, $2C_6$, $2C_8$, C_9, $2C_{12}$, $2C_{13}$, $2C_{14}$-H, CH_3). ^{13}C NMR (100 MHz, DMSO-d_6): δ (ppm) 167.4, 167.4, 152.5, 149.9, 137.3, 132.2, 132.0, 132.0, 116.9, 111.7, 111.6, 111.2, 71.8, 70.9, 65.5, 52.7, 52.1, 50.0, 43.6, 43.5, 43.2, 41.3, 41.0, 31.9, 30.5, 26.8, 19.1. HRMS (ESI) *m/z* calcd for $C_{27}H_{36}Cl_2NO_5$ $[M+H]^+$ 524.1965, found 524.1957.

4.1.2.3 Compound ***13a.*** Yellow oil, yield: 35%. ^{1}H NMR (400 MHz, DMSO-d_6): δ (ppm) 7.76 (4H, m, Ar-H), 7.39 (1H, dd, *J* = 15.7, 3.1 Hz, C_3-H), 6.82 (4H, m, Ar-H), 5.83 (1H, m, C_{11}-H), 5.58 (1H, d, *J* = 15.74 Hz, C_2-H), 5.53 (1H, d, *J* = 10.17 Hz, C_{10}-H), 5.23−5.33 (2H, m, C_4, C_7-H), 4.75 (1H, m, C_{15}-H), 3.76−3.77 (16H, m, -NCH_2CH_2Cl), 0.77−2.80 (15H, m, C_5, $2C_6$, $2C_8$, C_9, $2C_{12}$, C_{13}, $2C_{14}$-H, CH_3). ^{13}C NMR (100 MHz, DMSO-d_6): δ(ppm) 166.1, 165.3, 165.0, 152.1, 150.7, 149.5, 136.5, 132.9, 131.7, 131.6, 131.5, 131.5, 119.2, 117.9, 117.3, 112.1, 111.8, 111.58, 111.58, 76.2, 71.8, 71.1, 52.2, 52.2, 52.1, 52.1, 50.4, 49.4, 44.6, 43.6, 41.3, 41.3, 41.3, 41.3,

38.5, 33.9, 26.8, 21.0. HRMS (ESI) *m/z* calcd for $C_{38}H_{47}Cl_4N_2O_6$ $[M+H]^+$ 767.2183, found 767.2174.

4.1.2.4 Compound ***11b*****.** Yellow oil, yield: 32%. ^{1}H NMR (400 MHz, DMSO-d_6): δ (ppm) 7.27 (1H, dd, *J* = 15.8, 3.3 Hz, C_3-H), 7.04 (2H, d, *J* = 8.6 Hz, Ar-H), 6.68 (2H, d, *J* = 8.6 Hz, Ar-H), 5.71 (1H, m, C_{11}-H), 5.59 (1H, dd, *J* = 15.8, 1.6 Hz, C_2-H), 5.20−5.26 (2H, m, C_4, C_{10}-H), 4.75 (1H, m, C_{15}-H), 4.56 (1H, s, OH), 4.07 (1H, m, C_7-H), 3.70 (8H, m, -NCH_2CH_2Cl), 0.74−2.49 (21H, m, -$CH_2CH_2CH_2$-, C_5, 2C_6, 2C_8, C_9, 2C_{12}, 2C_{13}, 2C_{14}-H, CH_3). ^{13}C NMR (100 MHz, DMSO-d_6): δ(ppm) 172.4, 165.4, 149.3, 145.0, 137.2, 130.2, 129.9, 129.8, 129.8, 117.4, 112.4, 112.4, 76.4, 71.7, 70.8, 52.7, 52.7, 49.6, 43.4, 43.3, 41.6, 41.6, 40.9, 33.9, 33.8, 33.4, 31.8, 27.2, 26.8, 21.1. HRMS (ESI) *m/z* calcd for $C_{30}H_{42}Cl_2NO_5$ $[M+H]^+$ 566.2435, found 566.2391.

4.1.2.5 Compound ***12b*****.** Yellow oil, yield: 19%. ^{1}H NMR (400 MHz, DMSO-d_6): δ (ppm) 7.76 (2H, d, *J* = 9.0 Hz, Ar-H), 7.37 (1H, dd, *J* = 15.6, 3.0 Hz, C_3-H), 6.84 (2H, d, *J* = 9.1 Hz, Ar-H), 5.71−5.78 (2H, m, H-2, C_{11}-H), 5.20−5.26 (3H, m, OH, C_{10}-H, C_7-H), 4.72 (1H, m, C_{15}-H), 4.05 (1H, m, C_4-H), 3.76−3.81 (8H, m, -NCH_2CH_2Cl), 0.75−2.33 (21H, m, -$CH_2CH_2CH_2$-, C_5, 2C_6, 2C_8, C_9, 2C_{12}, 2C_{13}, 2C_{14}-H, CH_3). ^{13}C NMR (100 MHz, DMSO-d_6): δ(ppm) 166.1, 165.7, 154.7, 150.7, 137.0, 131.5, 131.5, 130.6, 129.2, 117.0, 111.7, 111.7, 75.6, 74.5, 71.4, 56.5, 56.5, 52.8, 52.2, 52.2, 43.2, 41.3, 41.3, 39.1, 33.9, 31.9, 30.5, 26.9, 21.2, 19.0. HRMS (ESI) *m/z* calcd for $C_{30}H_{42}Cl_2NO_5$ $[M+H]^+$ 566.2435, found 566.2417.

4.1.2.6 Compound ***13b*****.** Yellow oil, yield: 19%. ^{1}H NMR (400 MHz, DMSO-d_6): δ (ppm) 7.27 (1H, dd, *J* = 15.8, 3.2 Hz, C_3-H), 7.01 (4H, dd, *J* = 8.5, 3.0 Hz, Ar-H), 6.64 (4H, dd, *J* = 8.7, 3.1 Hz, Ar-H), 5.73−5.81 (1H, m, C_{11}-H), 5.61 (1H, d, *J* = 15.66 Hz, C_2-H), 5.32 (1H, d, *J* = 9.7 Hz, C_{10}-H), 5.20 (1H, dd, *J* = 15.2, 9.7 Hz, C_4-H), 5.04 (1H, m, C_7-H), 4.75 (1H, m, C_{15}-H), 3.69 (16H, m, -NCH_2CH_2Cl), 0.75−2.46

(27H, m, $CH_2CH_2CH_2$, C_5, $2C_6$, $2C_8$, C_9, $2C_{12}$, $2C_{13}$, $2C_{14}$-H, CH_3). ^{13}C NMR (100 MHz, DMSO-d_6): δ (ppm) 172.8, 172.3, 165.4, 149.0, 145.0, 145.0, 136.3, 131.1, 130.0, 129.8, 129.7, 129.7, 129.7, 129.7, 117.6, 112.4, 112.4, 112.3, 112.3, 76.1, 75.2, 71.8, 52.7, 52.7, 52.7, 52.7, 49.9, 42.9, 41.6, 41.6, 41.6, 41.6, 41.6, 41.6, 38.1, 33.9, 33.7, 33.7, 33.3, 31.8, 27.2, 27.1, 26.8, 21.1. HRMS (ESI) *m/z* calcd for $C_{44}H_{59}Cl_4N_2O_6$ $[M+H]^+$ 851.3122, found 851.3101.

4.1.2.7 Compound ***11c*****.** Yellow oil, yield: 21%. ^1H NMR (400 MHz, DMSO-d_6): δ (ppm): 7.24 (1H, dd, J = 15.8, 3.1 Hz, C_3-H), 7.0 (2H, d, J = 8.6 Hz, Ar-H), 6.65 (2H, d, J = 8.7 Hz, Ar-H), 5.72 (1H, m, C_{11}-H), 5.62 (1H, dd, J = 15.8, 1.7 Hz, C_2-H), 5.15−5.25 (2H, m, C_4-H, C_{10}-H), 4.72 (1H, m, C_{15}-H), 4.37 (1H, m, -NH), 4.05 (1H, m, C_7-H), 3.69 (8H, m, -NCH_2CH_2Cl), 3.58 (3H, s, OCH_3), 0.69−2.89 (22H, m, -$COCH_2CH_2CO$-, -$ArCH_2CHNCO$-, C_5, $2C_6$, $2C_8$, C_9, $2C_{12}$, $2C_{13}$, $2C_{14}$-H, CH_3). ^{13}C NMR (100 MHz, DMSO-d_6): δ(ppm) 172.7, 171.8, 171.3, 165.5, 149.0, 145.4, 137.2, 130.6, 130.6, 130.2, 125.6, 117.5, 112.1, 112.1, 76.6, 71.6, 70.8, 54.4, 52.6, 52.6, 52.2, 49.5, 43.4, 43.3, 41.6, 41.6, 40.7, 36.4, 33.8, 31.8, 30.0, 29.2, 26.9, 21.1. HRMS (ESI) *m/z* calcd for $C_{34}H_{46}Cl_2N_2O_8Na$ $[M+Na]^+$ 703.2523, found 703.2451.

4.1.2.8 Compound ***12c*****.** Yellow oil, yield: 6%. ^1H NMR (400 MHz, DMSO-d_6): δ (ppm) 7.34 (1H, dd, J = 15.5, 2.9 Hz, C_3-H), 7.03 (2H, d, J = 8.6 Hz, Ar-H), 6.64 (2H, d, J = 8.7 Hz, Ar-H), 5.67−5.76 (2H, m, C_{11}-H, C_2-H), 5.19 (1H, m, OH), 5.13 (1H, m, C_{10}-H), 4.97 (1H, m, C_7-H), 4.71(1H, m, C_{15}-H), 4.35 (1H, m, -NH), 3.99 (1H, m, C_4-H), 3.69 (8H, m, -NCH_2CH_2Cl), 3.58 (3H, s, OCH_3), 0.74−2.88 (22H, m, -$COCH_2CH_2CO$-, -$ArCH_2CHNHCO$-, C_5, $2C_6$, $2C_8$, C_9, $2C_{12}$, $2C_{13}$, $2C_{14}$-H, CH_3). ^{13}C NMR (100 MHz, DMSO-d_6): δ(ppm) 172.7, 172.3, 171.3, 166.1, 154.5, 145.4, 136.8, 130.5, 130.5, 130.5, 125.6, 116.9, 112.1, 112.1, 75.4, 74.5, 71.4, 54.4, 52.6, 52.6, 52.3, 52.2, 52.2, 43.2, 41.6, 41.6, 41.6, 38.6, 36.3, 33.9, 31.9, 29.6, 26.9, 21.2. HRMS (ESI)

m/z calcd for $C_{34}H_{46}Cl_2N_2O_8Na$ $[M+Na]^+$ 703.2523, found 703.2457.

4.1.2.9 Compound ***13c*****.** Yellow oil, yield: 24%. ^{1}H NMR (400 MHz, DMSO-d_6): δ (ppm) 7.23 (1H, dd, J = 15.8, 3.1 Hz, C_3-H), 7.03 (4H, d, J = 8.5 Hz, Ar-H), 6.64 (4H, d, J = 8.4 Hz, Ar-H), 5.75 (1H, m, C_{11}-H), 5.64 (1H, dd, J = 15.8, 1.5 Hz, C_2-H), 5.17−5.24 (2H, m, C_4, C_{10}-H), 4.98 (1H, m, C_7-H), 4.73 (1H, m, C_{15}-H), 4.33−4.40 (2H, m, -NH), 3.69 (16H, m, -NCH_2CH_2Cl), 3.57−3.58 (6H, s, -OCH_3), 0.74−2.89 (29H, m, -$COCH_2CH_2CO$-, -$ArCH_2CHNCO$-, C_5, $2C_6$, $2C_8$, C_9, $2C_{12}$, $2C_{13}$, $2C_{14}$-H, CH_3). ^{13}C NMR (100 MHz, DMSO-d_6): δ (ppm) 172.6, 172.6, 172.2, 171.7, 171.3, 171.3, 165.4, 148.6, 145.4, 145.4, 136.4, 131.1, 130.6, 130.6, 130.6, 130.6, 125.6, 125.6, 117.7, 112.1, 112.1, 112.1, 112.1, 76.3, 75.2, 71.6, 54.4, 54.4, 52.6, 52.6, 52.6, 52.6, 52.2, 52.2, 49.6, 43.0, 41.6, 41.6, 41.6, 41.6, 41.6, 41.6, 37.8, 36.4, 36.4, 33.9, 31.8, 30.0, 30.0, 29.5, 29.2, 21.1. HRMS (ESI) m/z calcd for $C_{52}H_{69}Cl_4N_4O_{12}$ $[M+H]^+$ 1081.3661, found 1081.3552.

4.2 Stability of ***11a***

Compound **11a** was dissolved in culture medium to a final concentration of 100 μM from 50 mM stock solution in DMSO. The solutions were incubated at 37 ^{o}C. An aliquot (20 μL) of the incubation mixture was taken out at different time points (0, 1, 2, 3, 4, 5, 6, 8, 12, 24 h). and the component were analyzed by HPLC equipped with a C_{18} reverse phase column (Shimadzu, LC-6 AD) with the flow rate of 0.5 mL/min methanol-water (60 : 40−100 : 0) and detection at UV 230 nm.

4.3 MTT assay

The antiproliferative activities were determined by the MTT method. The assay was performed in 96-well plates. Cells were added to each well and incubated for 24 h at 37 ^{o}C in a humidified atmosphere of 5% CO_2. Then cells were incubated in the presence or absence of test compounds. After 72 h, 20 μL MTT solution (5 mg/mL)

per well was added to each cultured medium, which was incubated for another 4 h. Then, DMSO (150 μL) was added to each well and the plates were shaken for 10 min at room temperature. After that, the OD of each well was measured on a Microplate Reader (BIO-RAD) at the wavelength of 570 nm. In these experiments, the negative reference was 0.1% DMSO. BFA, nitrogen mustards and 5-FU were used as the positive reference. The IC_{50} values were calculated according to the inhibition ratios.

4.4 Cell cycle analysis

Cell cycle effects were tested by flow cytometry with PI (KGA511, KeyGEN Biotech, Nanjing, China). Bel-7402 cells were plated in 6-well plates and incubated at 37 ^{o}C for 24 h. Cells were then incubated with **11a** at certain concentrations. After 24 h, cells were centrifuged and fixed in 70% ethanol at 4 ^{o}C overnight and resuspended in PBS containing 100 μL RNase A and 400 μL PI. Cellular DNA content, for cell cycle distribution analysis, was measured using a flow cytometer (FACS Calibur Becton–Dickinson).

4.5 Hoechst 333258 staining

The nuclear morphological modifications were analyzed by fluorescent microscopy using Hoechst staining. In this experiment, Bel-7402 cells were seeded on 6-well plates, with 2 mL of medium. Following 24 h of incubation, compound **11a** was added at indicated concentrations and cells were incubated again for a period of 48 h. Cells were harvested by mild trypsinization, collected by centrifugation and washed twice with PBS. Cells were then stained with 500 μL of Hoechst solution (2 mg/mL in PBS) (Keygen, Nanjing, China) for 15 min at room temperature, in darkness. Following incubation cells were washed with PBS, mounted in a slide and observed with a fiuorescent microscope with a DAPI filter.

4.6 Cell apoptosis assay

Apoptosis was analyzed using Annexin V and PI double staining by flow cytometry according to the manufacturer's instructions (KGA1024, KeyGEN Biotech, Nanjing, China) in order to detect apoptotic cells. The Bel-7402 cells were seeded in 6-well plates to grow overnight, and then treated with or without **11a** at indicated concentrations for 24 h. Cells were then washed twice in PBS and resuspended in Annexin V binding buffer. Annexin V-FITC was then added and the mixture was incubated for 15 min under dark conditions at 25 ^{o}C. PI was added just prior to acquisition. The percentage of cells positive for PI and/or Annexin V-FITC was reported inside the quadrants.

4.7 Mitochondrial membrane potential assay

Briefly, Bel-7402 cells were incubated with **11a** or vehicle for 24 h, and then washed with PBS and stained with JC-1 dye under dark conditions according to the manufacturer's instruction (KGA601, KeyGEN Biotech, Nanjing, China). The percentage of cells with healthy or collapsed mitochondrial membrane potentials was monitored by flow cytometry analysis.

4.8 Western blot assay

Bel-7402 cells were incubated with **11a** at the indicated concentrations for 72 h. The cells were harvested and lysed using lysis buffer, and the solution was centrifuged at 14,000 g for 10 min at 4 ^{o}C. Then the protein concentrations were determined, and individual cell lysates (25 μg per lane) were separated by sodium dodecyl sulfate polyacrylamide gel electrophoresis (10% gel, SDS-PAGE) and transferred onto nitrocellulose membranes. After being blocked with 5% fat-free milk, the target proteins in the membranes were probed with monoclonal antibodies against Bcl-2, Bax, cyto-*c*, caspase-9, -3, p53 and GAPDH (KeyGEN Biotech, Nanjing, China) at 4 ^{o}C overnight, respectively. The bound antibodies were detected by appropriate second

antibodies and visualized using an enhanced chemiluminescent reagent. The relative levels of each signaling event to control GAPDH were determined by densimetric scanning.

Acknowledgment

This work was financially supported by the National Natural Science Foundation of China (41576136), Project Funded by China Post Doctoral Science Foundation (2017T100186), Natural Science Foundation of Liaoning Province (20170540858), General Scientific Research Projects of Department of Education in Liaoning Province (2017LQN05), and Career Development Support Plan for Young and Middle-aged Teachers in Shenyang Pharmaceutical University.

References

[1] C. Allemani, H.K. Weir, H. Carreira, R. Harewood, D. Spika, X.-S. Wang, F. Bannon, J.V. Ahn, C.J. Johnson, A. Bonaventure, R. Marcos-Gragera, C. Stiller, G. A. e Silva, W.-Q. Chen, O.J. Ogunbiyi, B. Rachet, M.J. Soeberg, H. You, T. Matsuda, M. Bielska-Lasota, H. Storm, T.C. Tucker, M.P. Coleman, Lancet 385 (2015) 977−1010.

[2] A.B. Ryerson, C.R. Eheman, S.F. Altekruse, J.W. Ward, A. Jemal, R.L. Sherman, S.J. Henley, D. Holtzman, A. Lake, A. Noone, R.N. Anderson, J.-M. Ma, K.N. Ly, K.A. Cronin, L. Penberthy, B.A. Kohler, Annual report to the nation on the status of cancer, 1975−2012, featuring the increasing incidence of liver cancer, Cancer 122 (2016) 1312−1337.

[3] W.-Q. Chen, R.-S. Zheng, P.D. Baade, S.-W. Zhang, H.-M Zeng, F. Bray, A. Jemal, X.-Q. Yu, J. He, Cancer statistics in China, 2015, CA-Cancer J. Clin. 66

(2016) 115−132.

[4] T. Rodrigues, D. Reker, P. Schneider, G. Schneider, Counting on natural products for drug design, Nat. Chem. 8 (2016) 531−541.

[5] D.J. Newman, G.M. Cragg, Natural products as sources of new drugs from 1981 to 2014, J. Nat. Prod. 79 (2016) 629−661.

[6] J.-L. Moon, S.-Y. Kim, S.-W. Shin, J.-W. Park, Regulation of brefeldin A-induced ER stress and apoptosis by mitochondrial $NADP^+$-dependent isocitrate dehydrogenase, Biochem. Biophys. Res. Commun. 417 (2012) 760−764.

[7] T. Toda, M. Watanabe, J. Kawato, M.E. Kadin, M. Higashihara, T. Kunisada, K. Umezawa, R. Horie, Brefeldin A exerts differential effects on anaplastic lymphoma kinase positive anaplastic large cell lymphoma and classical Hodgkin lymphoma cell lines, Br. J. Haematol. 170 (2015) 837−846.

[8] H.-R. Huang, T. Liu, J.-X. Guo, L. Yu, X.-F. Wu, Y. He, D.-L. Li, J.-L. Liu, K. Zhang, X. Zheng, S. Goodin, Brefeldin A enhances docetaxel-induced growth inhibition and apoptosis in prostate cancer cells in monolayer and 3D cultures, Bioorg. Med. Chem. Lett. 27 (2017) 2286−2291.

[9] P.F. South, K.M. Harmeyer, N.D. Serratore, S.D. Briggs, H3K4 methyltransferase set1 is involved in maintenance of ergosterol homeostasis and resistance to brefeldin A, Proc. Natl. Acad. Sci. 110 (2013) E1016−E1025.

[10] S. Rajamahanty, C. Alonzo, S. Aynehchi, M. Choudhury, S. Konno, Growth inhibition of androgen-responsive prostate cancer cells with brefeldin A targeting cell cycle and androgen receptor, J. Biomed. Sci. 17 (2010) 5.

[11] C. Grose, D. J. Klionsky, Alternative autophagy, brefeldin A and viral trafficking pathways, Autophagy 12 (2016) 1−2.

[12] N.O. Anadu, V.J. Davisson, M. Cushman, Synthesis and anticancer activity of

brefeldin A ester derivatives, J. Med. Chem. 49 (2006) 3897−3905.

[13] Y.-K. Wu, J. Gao, Total synthesis of (+)-brefeldin A, Org. Lett. 10 (2008) 1533−1536.

[14] M. Fuchs, A. Fürstnera, *trans*-Hydrogenation: applicationtoa concise and scalable synthesis of brefeldin A, Angew. Chem. Int. Ed. 54 (2015) 3978−3982.

[15] A. Colanzi, G. Grimaldi, G. Catara, C. Valente, C. Cericola, P. Liberali, M. Ronci, V.S. Lalioti, A. Bruno, A.R. Beccari, A. Urbani, A.D. Flora, M. Nardini, M. Bolognesi, A. Luini, D. Corda, Molecular mechanism and functional role of brefeldin A-mediated ADP-ribosylation of CtBP1/BARS, Proc. Natl. Acad. Sci. 110 (2013) 9794−9799.

[16] Y. Ito, T. Uemura, K. Shoda, M. Fujimoto, T. Ueda, A. Nakano, *cis*-Golgi proteins accumulate near the ER exit sites and act as the scaffold for Golgi regeneration after brefeldin A treatment in tobacco BY-2 cells, Mol. Biol. Cell. 23 (2012) 3203−3214.

[17] S.-A. Lee, Y.-J. Kim, C.-S. Lee, Brefeldin A induces apoptosis by activating the mitochondrial and death receptor pathways and inhibits focal adhesion kinase-mediated cell invasion, Basic Clin. Pharmacol. Toxicol. 113 (2013) 329−338.

[18] E. Wallen, R.G. Sellers, D.M. Peehl, Brefeldin A induces p53-independent apoptosis in primary cultures of human proststic cancer cells, J. Urol. 164 (2000) 836−841.

[19] C.-N. Tseng, Y.-R. Hong, H.-W. Chang, T.-J. Yu, T.-W. Hung, M.-F. Hou, S.S.F. Yuan, C.-L. Cho, C.-T. Liu, C.-C. Chiu, C.-J. Huang, Brefeldin A reduces anchorage-independent survival, cancer stem cell potential and migration of MDA-MB-231 human breast cancer cells, Molecules 19 (2014) 17464−17477.

[20] S. Förster, E. Persch, O. Tverskoy, F. Rominger, G. Helmchen, C. Klein, B. Gönen, B. Brügger, Syntheses and biological properties of brefeldin analogues, Eur. J. Org. Chem. (2011) 878−891.

[21] S. Kikuchi, K. Shinpo, S. Tsuji, I. Yabe, M. Niino, K. Tashiro, Brefeldin A-induced neurotoxicity in cultured spinal cord neurons, J. Neurosci. Res. 71 (2003) 591−599.

[22] J.-W. Zhu, H. Hori, H. Nojiri, T. Tsukuda, Z. Taira, Synthesis and activity of brefeldin A analogs as inducers of cancer cell differentiation and apoptosis, Bioorg. Med. Chem. Lett. 7 (1997) 139−144.

[23] J.-W. Zhu, H. Nagasawa, F. Nagura, S.B. Mohamad, Y. Uto, K. Ohkura, H, Hori, Elucidation of strict structural requirements of brefeldin A as an inducer of differentiation and apoptosis, Bioorg. Med. Chem. 8 (2000) 455−463.

[24] B.M. Fox, J.A. Vroman, P.E. Fanwick, M. Cushman, Preparation and evaluation of sulfide derivatives of the antibiotic brefeldin a as potential prodrug candidates with enhanced aqueous solubilities J. Med. Chem. 44 (2001) 3915−3924.

[25] K. Seehafer, F. Rominger, G. Helmchen, M. Langhans, D.G. Robinson, B. Ozata, B. Brugger, J.R.P.M. Strating, F.J.M. van Kuppeveld, C.D. Klein, Synthesis and biological properties of novel brefeldin A analogues, J. Med. Chem. 56 (2013) 5872−5884.

[26] L.F. Povirk, D.E. Shuker, DNA damage and mutagenesis induced by nitrogen mustards. Mutat. Res. 318 (1994) 205−226.

[27] S.-T. Xu, L.-L. Pei, C.-Q. Wang, Y.-K. Zhang, D.-H. Li, H.-Q. Yao, X.-M. Wu, Z.-S. Chen, Y.-J. Sun, J.-Y. Xu, Novel hybrids of natural oridonin-bearing nitrogen mustards as potential anticancer drug candidates, ACS Med. Chem. Lett. 5 (2014) 797−802.

[28] L.-M. Zhao, F.-Y. Ma, H.-S. Jin, S.-L. Zheng, Q. Zhong, G.-D. Wang, Design and synthesis of novel hydroxyanthraquinone nitrogen mustard derivatives as potential anticancer agents via a bioisostere approach, Eur. J. Med. Chem. 102 (2015) 303−309.

[29] Y.-Z. Xu, X.-Y. Gu, S.-J. Peng, J.-G. Fang, Y.-M. Zhang, D.-J. Huang, J.-J. Chen, K. Gao, Design, synthesis and biological evaluation of novel sesquiterpene mustards as potential anticancer agents, Eur. J. Med. Chem. 94 (2015) 284−297.

[30] X. Hu, Y. Wang, J.-J. Xue, T. Han, R.-W. Jiao, Z.-L. Li, W.-W. Liu, F.-X. Xu, H.-M. Hua, D.-H. Li, Design and synthesis of novel nitrogen mustard-evodiamine hybrids with selective antiproliferative activity, Bioorg. Med. Chem. Lett. 27 (2017) 4989−4993.

[31] R.C. Elderfield, T.-K. Liao, Synthesis of potential anticancer agents. XII. nitrogen mustards from *p*-aminobenzoic acid derivatives, J. Org. Chem. 26 (1961) 4996−4997.

[32] M.K. Kim, K.S. Park, C. Lee, H.R. Park, H. Choo, Y. Chong, Enhanced stability and intracellular accumulation of quercetin by protection of the chemically or metabolically susceptible hydroxyl groups with a pivaloxymethyl (POM) promoiety, J. Med. Chem. 53 (2010) 8597−8607.

[33] D.V. Krysko, T.V. Berghe, E. Parthoens, K. D'Herde, P. Vandenabeele, Methods for distinguishing apoptotic from necrotic cells and measuring their clearance, Methods Enzymol. 442 (2008) 307−341.

[34] D.R. Green, J.C. Reed, Mitochondria and apoptosis, Science 281 (1998) 1309−1312.

[35] J.F.R. Kerr, A.H. Wyllie, A.R. Currie, Apoptosis: a basic biological phenomenon with wide-ranging implications in tissue kinetics, Br. J. Cancer 26 (1972)

239−257.

[36] G.M. Cohen, Caspases : the executioners of apoptosis, Biochem. J. 326 (1997) 1−16.

[37] N.B. Blatt, G.D. Glick, Signaling pathways and effector mechanisms pre-programmed cell death, Bioorg. Med. Chem. 9 (2001) 1371−1384.

[38] J.S. Fridman, S.W. Lowe, Control of apoptosis by p53, Oncogene 22 (2003) 9030−9040.

Table 1

Effects of BFA derivatives on cell viability against different cell lines.

Compound	IC_{50} (μM)[a]					
	HL-60	PC-3	Bel-7402	Bel-7402/5-FU	L-O2	SI[b]
11a	4.48 ± 0.28	9.37 ± 0.49	0.25 ± 0.02	0.84 ± 0.02	9.74 ± 0.36	38.9
12a	8.25 ± 0.80	10.57 ± 0.84	1.45 ± 0.12	4.05 ± 0.30	9.51 ± 0.42	6.6
13a	9.31 ± 0.45	18.54 ± 1.56	6.30 ± 0.27	15.30 ± 1.05	17.32 ± 0.80	2.7
11b	12.55 ± 0.63	1.37 ± 0.12	1.93 ± 0.16	8.35 ± 0.40	29.58 ± 0.79	15.3
12b	34.68 ± 2.45	6.84 ± 0.49	4.86 ± 0.48	13.85 ± 0.96	15.47 ± 1.26	3.2
13b	67.43 ± 2.76	20.36 ± 1.32	7.25 ± 0.34	15.63 ± 0.72	19.47 ± 0.84	2.7
11c	1.52 ± 0.04	14.46 ± 0.47	1.37 ± 0.07	4.60 ± 0.14	5.16 ± 0.23	3.8
12c	14.37 ± 1.22	17.58 ± 1.33	1.49 ± 0.13	3.05 ± 0.12	4.57 ± 0.25	3.1
13c	9.37 ± 0.48	32.54 ± 2.60	4.85 ± 0.26	7.47 ± 0.41	29.87 ± 1.47	6.2
4	12.36 ± 0.65	57.27 ± 2.40	46.45 ± 2.17	> 80	68.57 ± 2.08	1.5
7	6.02 ± 0.34	> 80	23.94 ± 1.34	> 80	32.86 ± 2.39	1.37
Chlorambucil	11.63 ± 0.42	40.35 ± 1.78	> 80	> 80	> 80	NC[d]
BFA	0.025 ± 0.002	0.068 ± 0.003	0.024 ± 0.001	0.82 ± 0.05	< 0.001	NC
5-FU	2.37 ± 0.20	23.86 ± 1.05	18.49 ± 1.20	> 80	NT[c]	

[a]IC_{50}: half inhibitory concentrations measured by the MTT assay. The values are expressed as averages ± standard deviations of three independent experiments. [b]SI: selectivity index. It was calculated as: $SI = IC_{50(L\text{-}O2)}/IC_{50(Bel\text{-}7402)}$. [c] NT: not tested. [d]NC: not calculated.

1. Legends of Fig. 1, Fig. 2, Fig. 3, Fig. 4, Fig. 5, Fig. 6, Fig. 7, Fig. 8, Scheme 1 and Scheme 2

Fig. 1. The chemical structures of BFA and some of its derivatives.

Fig. 2. The chemical structures of some reported natural product/nitrogen mustard hybrids.

Fig. 3. HPLC of (a) BFA and **11a** in MeOH, (b) **11a** in cell-free culture medium (cDMEM) after incubation for 1, 6, 12 and 24 h.

Fig. 4. Cell cycle analysis of **11a** in Bel-7402 cells by flow cytometry.

Fig. 5. Hoechst staining of **11a** in Bel-7402 cells.

Fig. 6. Flow cytometry analysis of apoptosis induced by **11a** in Bel-7402 cells.

Fig. 7. 11a induced mitochondrial depolarization in Bel-7402 cells.

Fig. 8. 11a affected the expressions of the mitochondria pathway related proteins in Bel-7402 cells. Con is short for control.

Scheme 1. Synthesis of compounds **4** and **7**. Reagents and conditions: (a) ethylene oxide, H_2O, CH_3COOH, rt, 24 h; (b) $POCl_3$, 50 ^oC, 0.5 h; (c) 10% HCl, 12 h; (d) $SOCl_2$, MeOH, reflux, 12 h; (e) succinic anhydride, DMAP, DCM, rt, 18 h.

Scheme 2. Synthesis of compounds **11a**−**c**, **12a**−**c** and **13a**−**c**. Reagents and conditions: (a) TBSOTf, 2,6-lutidine, DCM, 0−25 ^oC, 3 h; (b) TBAF (1 eq.), THF, 0−25 ^oC, 24 h; (c) **4**, **7** or chlorambucil, EDCI, DMAP, DCM, rt, 24 h; (d) TBAF (7 eq.), THF, 0−25 ^oC, 20 h; (e) **4**, **7** or chlorambucil, EDCI, DMAP, DCM, rt, 12−24 h.

2. Graphics for Fig. 1, Fig. 2, Fig. 3, Fig. 4, Fig. 5, Fig. 6, Fig. 7, Fig. 8, Scheme 1 and Scheme 2

Figure 1

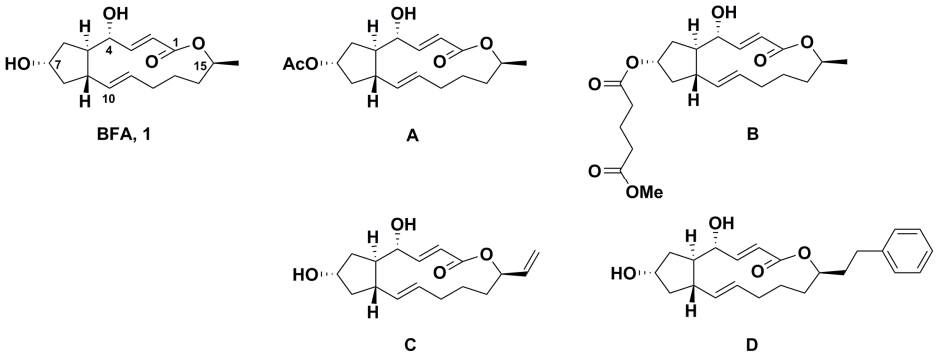

Figure 2

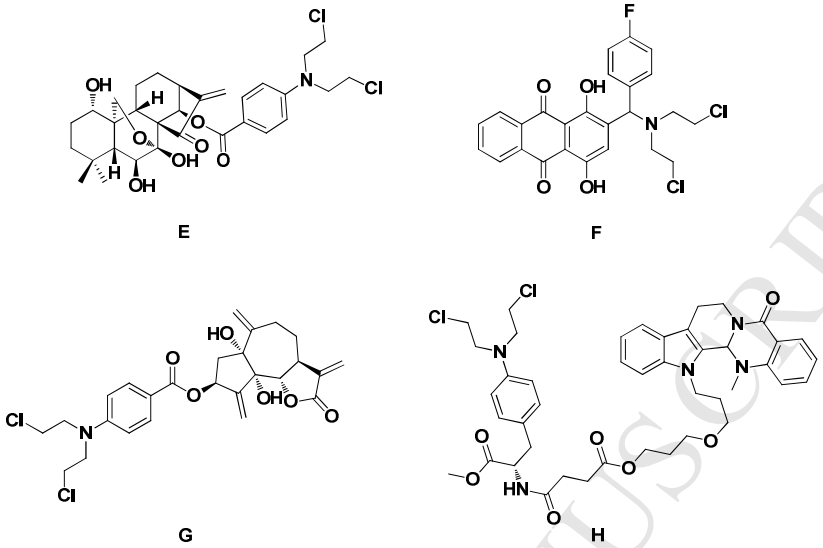

Figure 3

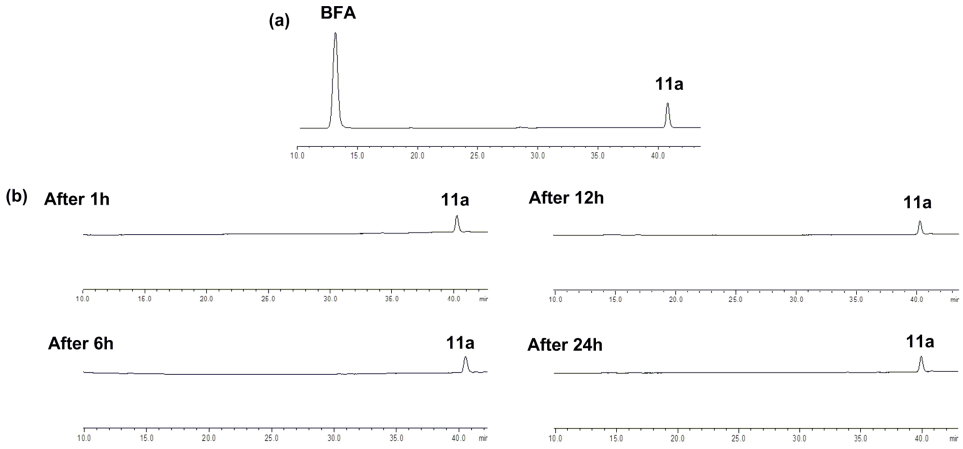

Figure 4

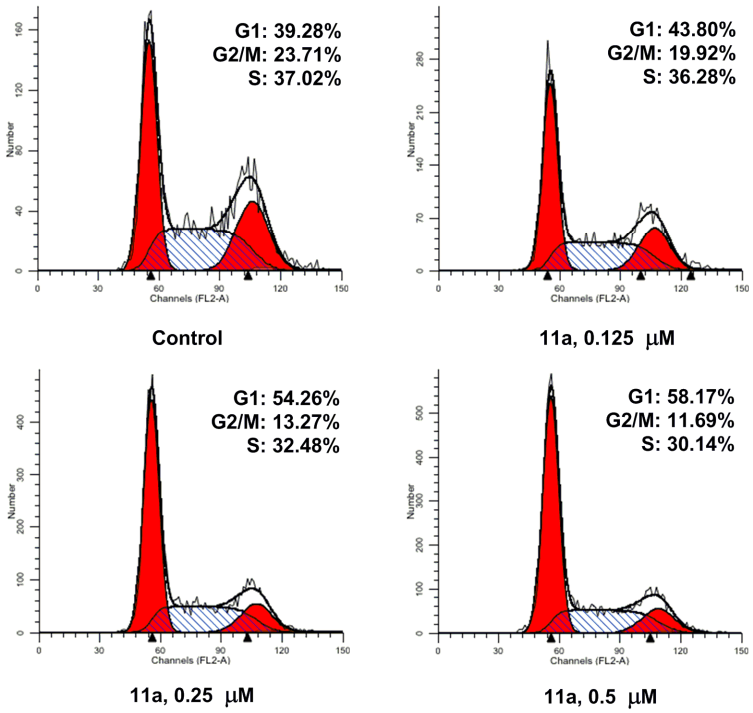

Figure 5

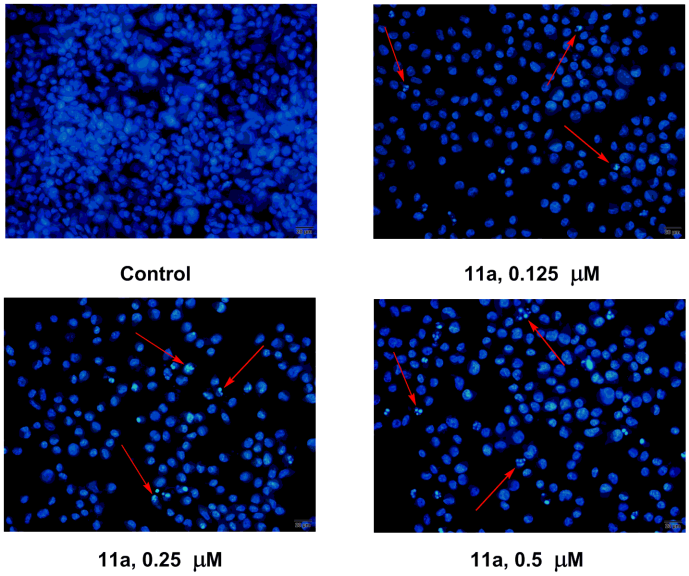

Figure 6

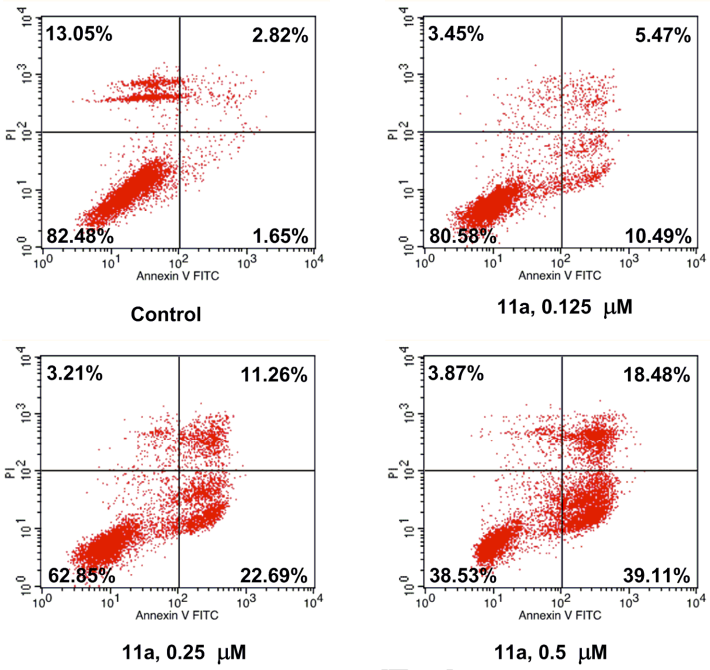

Figure 7

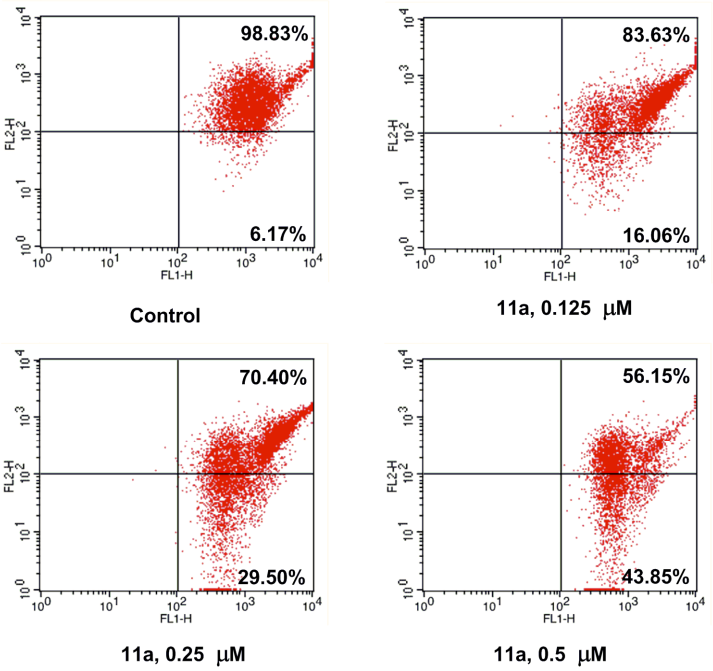

Figure 8

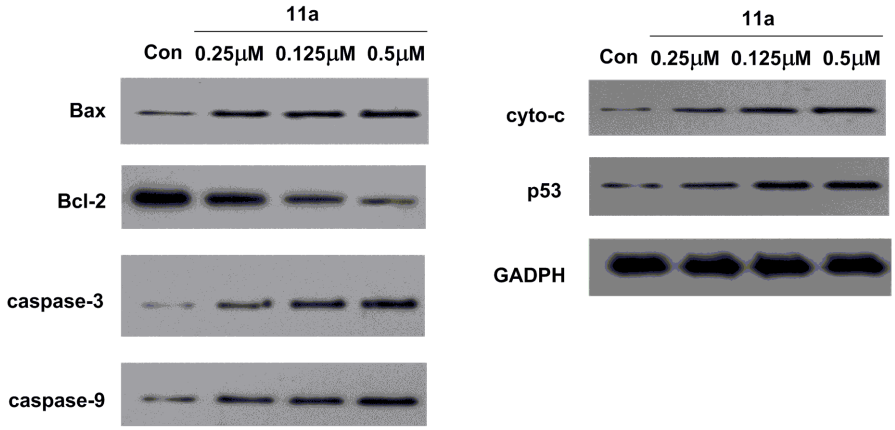

Scheme 1

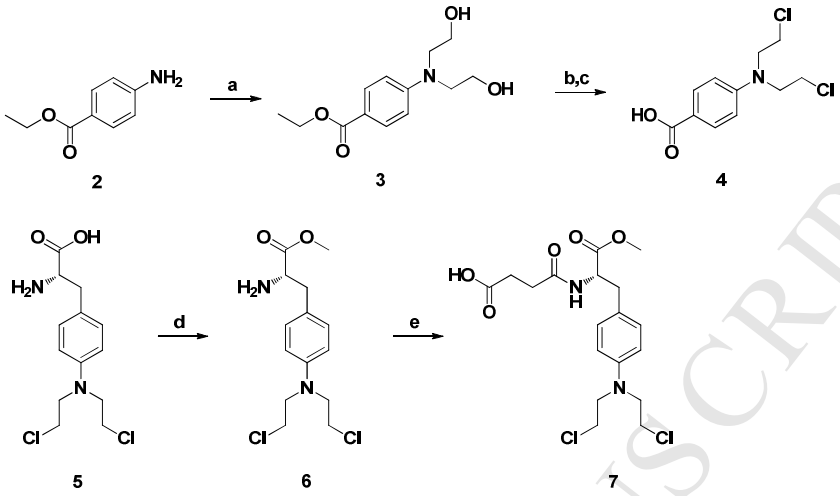

Scheme 2

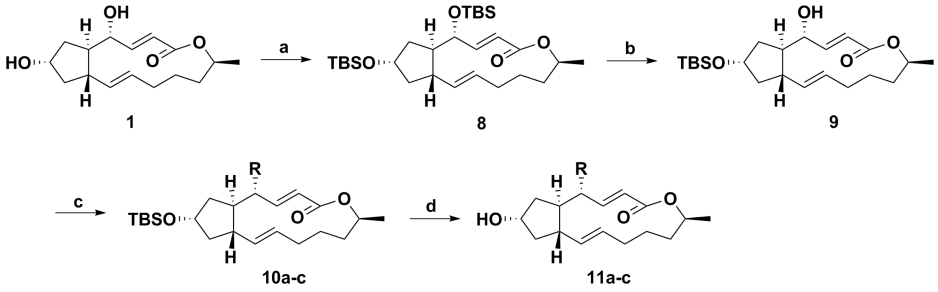

Highlights

Novel hybrids of brefeldin A and nitrogen mustards were designed and synthesized.
Some derivatives exhibited potent antiproliferative activity with low IC_{50} values.
Compound **11a** showed good selectivity between human normal and tumor liver cells.
11a induced apoptosis and arrest cell cycle at G1 phase in Bel-7402 cells.
11a induced Bel-7402 cells apoptosis via the mitochondria-dependent pathway.